Brachytherapy using Magnetic Field Sensing

Benjamin Chu
Automation Sciences Laboratory
University of California, Berkeley
Department of Electrical Engineering and Computer Sciences (EECS)
September 11, 2010

ABSTRACT

Brachytherapy provides a localized radiation treatment, with many advantages over conventional radiation treatments. However, this treatment is still under development. The current setup involves using a stud finder to sense a steerable needle, with limited results. Therefore, magnetic field sensing was tested. After filtering methods, the images produced from magnetic field sensing have less noise, and higher fidelity. However, the system is limited by a two centimeter detection range. Higher quality sensors and stronger magnets may improve the performance of magnetic field sensing.

Introduction:

Background Information

Brachytherapy is a form of radiation therapy where the radiation source is placed near the region needing treatment for a localized treatment effect. A radioactive seed is delivered inside the patient using steerable needles. The needle to deliver the radioactive seed has a bevel tip, which allows the needle to turn when inserted into the phantom tissue. This allows the needle to be steered to any location in the body while avoiding obstacles. The Berkeley Automation Sciences Laboratory has worked extensively on needle motion planning algorithms. There has also been ongoing work on developing an experimental setup to physically test these algorithms. The system should sense the position of the needle in three dimensions, while provide mechanical actuation for needle insertion and steering.

The basic sensing setup sweeps a household stud finder across the working space of the needle to locate the position of the needle, by measuring changes in the dielectric constant of the surface. However, there are many issues with using a stud finder as a sensor. With a better sensor, performance can be improved. Many sensors have the potential to improve performance over the existing stud sensor setup. The team at Johns Hopkins University has successfully implemented cameras. The idea of sensing a magnet placed at the tip of the needle was implemented, since this idea has not been tested before. Magnetic sensing is also able to image organs in opaque flesh for clinical trials [1] [2].

Magnetic Field Sensing

To avoid obstacles during needle steering, the length of the needle should follow the trajectory of the tip, such that the needle moves in the longitudinal direction. The flesh might flex as the needle is inserted, but the needle should remain in the same position relative to the surrounding flesh. Therefore, if the position of the tip is known, the position of the entire needle can be inferred. The improved setup to sense the needle involves mounting a magnet on the needle tip, and sensing its location using Hall-Effect sensors, in contrast to the existing system, which uses a stud sensor to directly measure the entire needle.

Methods

Steerable Needles

An experimental test bed was built, which is able to actuate and sense steerable needles. An aluminum structure was built and a transparent plastic sheet is used to separate the sensing equipment from the phantom tissue underneath. A needle made of a flexible material called nitinol, is used. To mimic the physical properties of flesh, a phantom tissue material called plastisol gel, is used.

An actuation system is used to both insert the needle into the phantom tissue and to rotate the needle in order to steer it. Stepper motors with angular feedback are used to finely control the amount of insertion and rotation into the flesh. A stepper motor driver is used to control the direction and displacement of the motor. A worm gear is used to convert rotational motion into the translational motion required for needle insertion. Figure 1 shows a picture of the needle insertion mechanism.

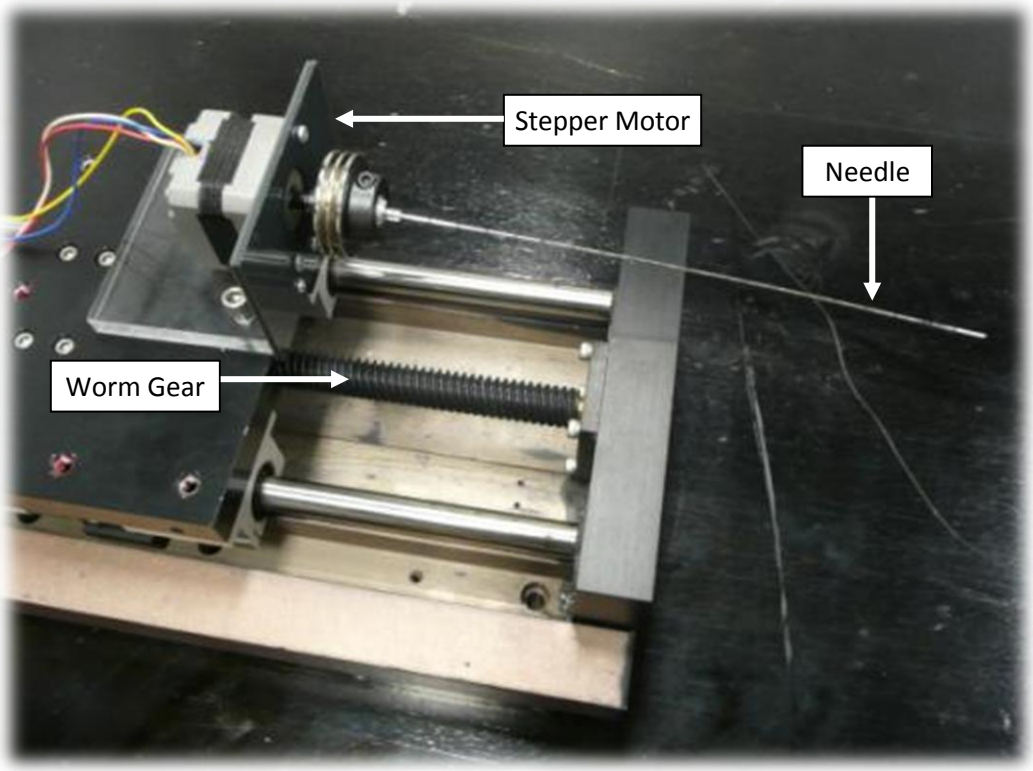

Figure 1: The steerable needle actuation system.

Hall-Effect Sensor Implementation

The magnetic source is a 0.125" Neodymium/Iron/Boron (NdFeB) cube. The magnetic sensor is an analog Hall-Effect sensor from Allegro Microsystems, mounted on the existing stud sensor. Wires were soldered on the leads, and insulated with shrink wrap. Analog filters were implemented on the breadboard using a simple resistor-capacitor circuit. The Hall-Effect sensor is attached to the bottom of the stud finder, to use the stud finder as a sweeping platform.

A mechanical sweeping mechanism was built to sweep the sensor along the working space of the needle. The system has two degrees of freedom, and allows the sensor to be swept across the entire work space of the needle. The actuation system includes a stepper motor to sweep the sensor in the longitudinal direction, using a belt attached to both the motor and the sensor. A servo motor with angular feedback sweeps the sensor in a lateral motion.

When the system is run, the servo motor is initially reset to an initial position, and starts to sweep in a clockwise direction. When it has completed sweeping, the servo will reset to its initial position, and the stepper motor will push the sensor forward one step. The servo motor will complete 10 sweeps before the stepper motor brings the servo motor back 10 steps to its initial position. The system will then reset and run the same motion. Figure 2 displays the various mechanical and electronic components of the system. Figure 3 shows

detail of the needle and magnet inside the phantom tissue. Figure 4 shows a close up view of the Hall-Effect sensor.

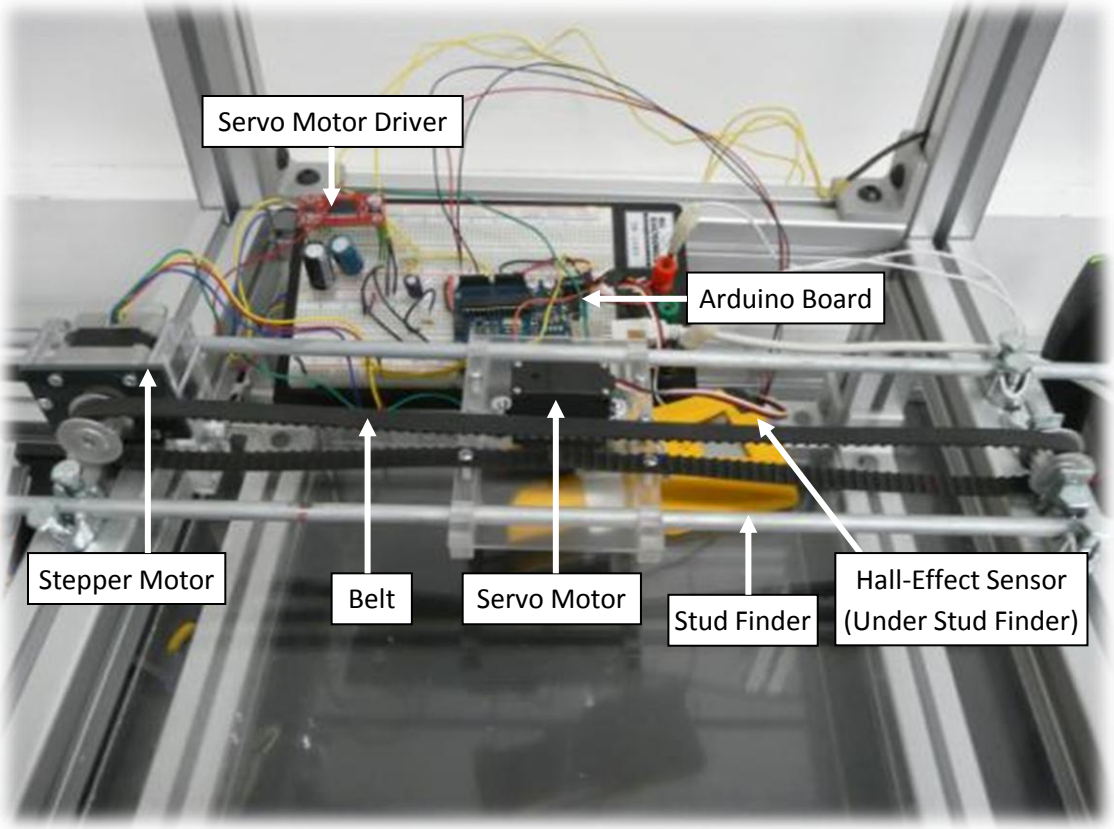

Figure 2: The test bed, with major parts labeled.

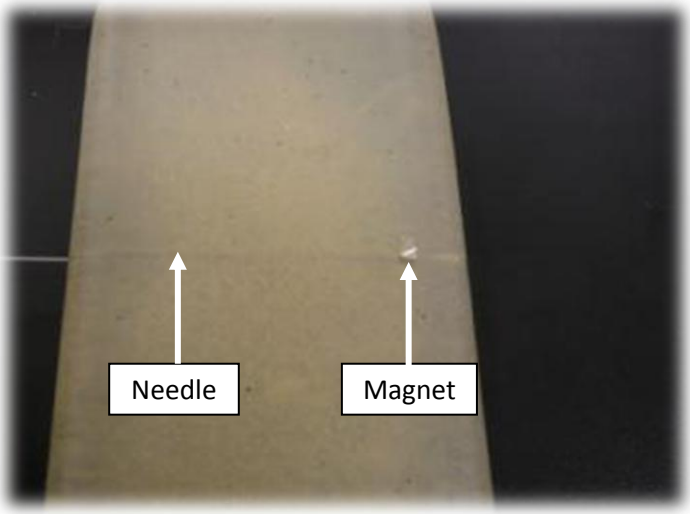

Figure 3: Detail of the needle in the phantom tissue, with a 0.125" magnet cube placed at the tip.

Figure 4: Detail on the Hall Effect Sensor.

Sensor Calibration

To calibrate the Hall-Effect sensor, data points of the voltage output of the sensor and the distance to the magnet were taken approximately every 0.2 cm. Distance measurements were provided by a centimeter ruler, which has tick marks at every millimeter. Voltage measurements were provided by the analog to digital converter (ADC) of the Arduino board, with a low pass filter to remove white noise. The plot of the sensor calibration is shown in Figure 5. Given the overall shape of the data points, a polynomial fit would be inaccurate, or be too complex to implement in software. Therefore, a piecewise curve of the form 1/x was used to account for the polarity of the magnetic field.

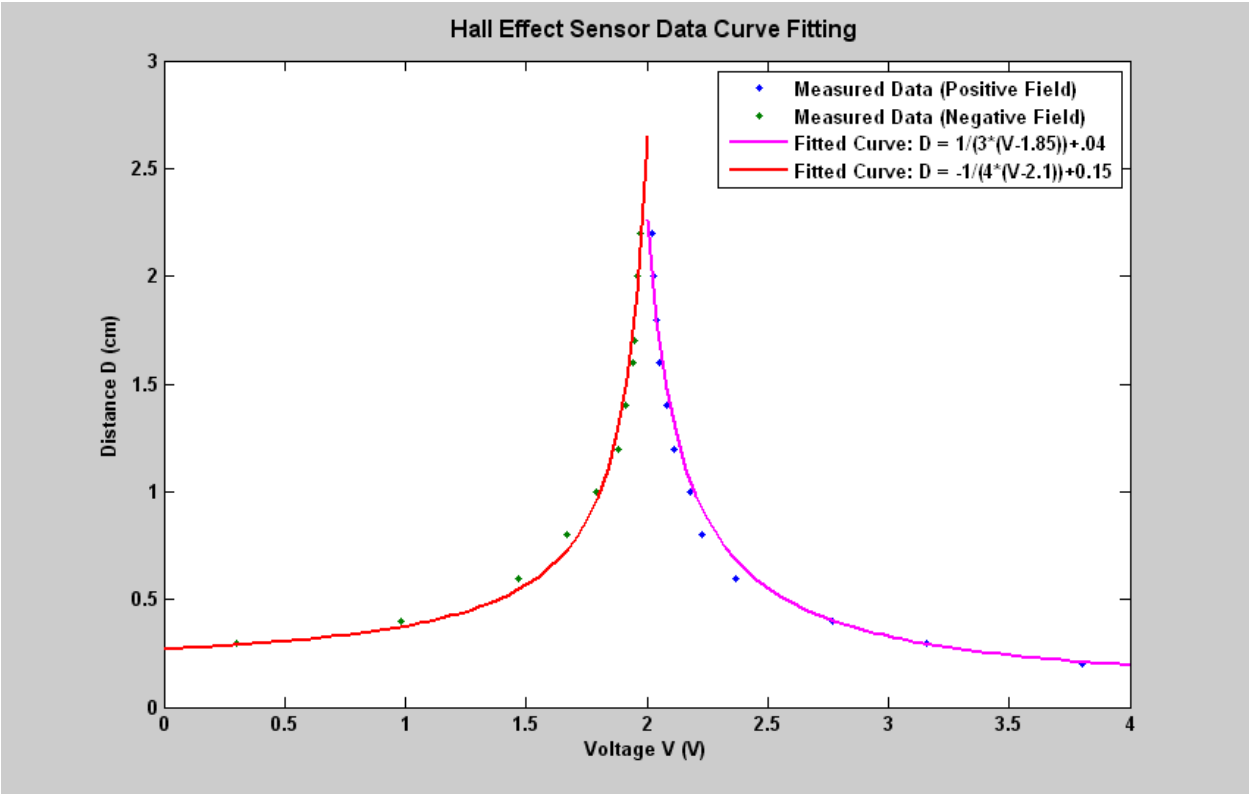

Figure 5: Plot of sensor calibration.

Sensor Filtering

To improve performance, both analog and digital filtering methods were implemented and tested. The digital filter is a simple two-point moving average algorithm of the form $a*V_i + (1-a)*V_{i-1}$, where $0 \leq a \leq 1$. The analog filter is a simple first order resistor-capacitor circuit, with a resistance of 100 Ω and a capacitance of 47 μF.

Software

An Arduino microcontroller was programmed in C++ to both control the needle actuation system and the needle sensing system. The Arduino software can be used in conjunction

with the Processing software, which uses serial communication with the microcontroller to draw a real-time image of the needle. Digital filtering methods were also implemented in software.

Currently, the Processing software plots the Hall-Effect sensor data in real-time as it is being swept. The strength of the magnetic field corresponds to the gray scale color of each plotted band. Black bands in the image correspond to no magnetic field, while lighter bands correspond to a detected magnetic field, where the lightness of the band is an indication of the magnitude of the field. The actual numeric values of the distance to the magnet can be outputted in real-time using serial communication, which will print out the current depth, along with the current angle and longitudinal position. After the entire sweep, the location of the needle tip will be the location where the depth reading was at a minimum.

Results

Error Analysis

Plots of the effects of digital and analog filtering on white noise are shown in Figures 6 and 7, respectively. All graphs were produced using the ADC on the Arduino board with a sampling period of 100 ms. The analog filter performs better in eliminating white noise of the sensor. However, adding digital filter can increase the precision of the readings, since the ADC of the microcontroller only has 10 bits of precision, while a float data-type is 32 bits long. The ideal solution is to combine both filtering methods. A magnet was placed near the sensor at 1 cm away to measure the sensor error. The error was fairly small, which is mostly under 0.1 cm. However, if the orientation of the magnet changes, there may be a significant deviation from these results.

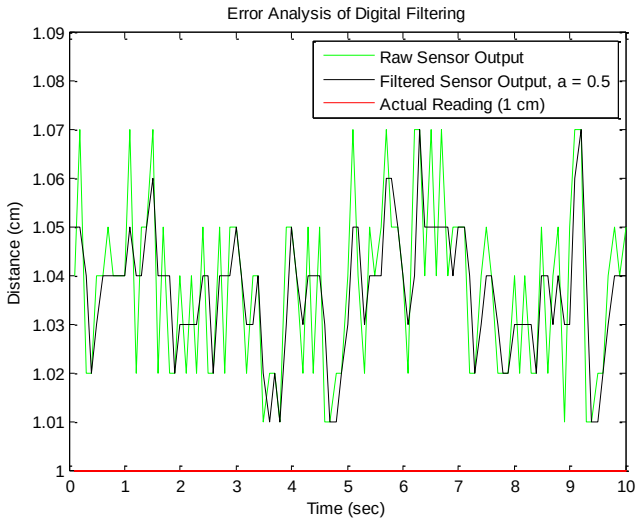

Figure 6: Error analysis with a digital LPF.

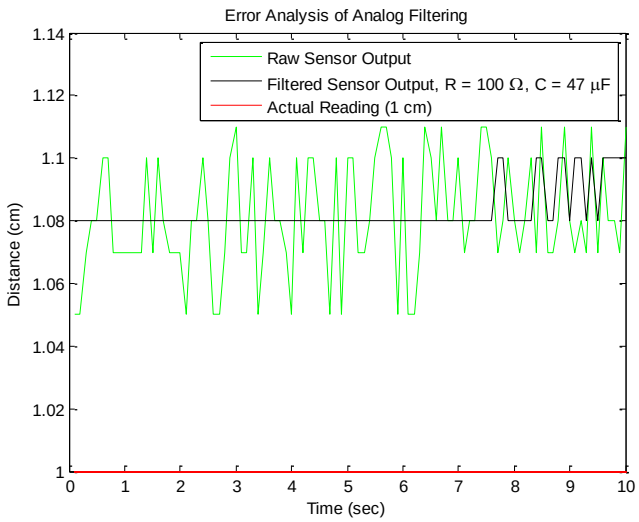

Figure 7: Error analysis with an analog LPF.

Effects of Filtering

The plots below compare a raw image without filtering (Figure 8), to a filtered image produced with analog and digital filtering methods (Figure 9). Without filtering, the plot is very noisy, with dark bands appearing periodically. However, once filtering methods are used, the dark bands are less visible in the image.

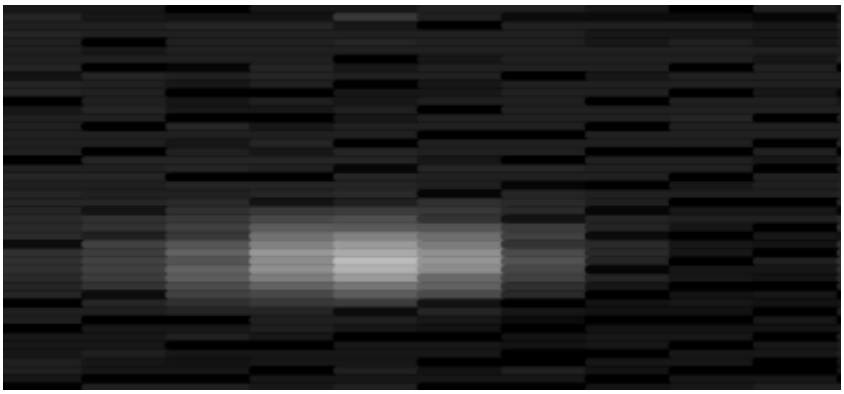

Figure 8: Image of the needle tip using the Hall-Effect sensor, without filtering.

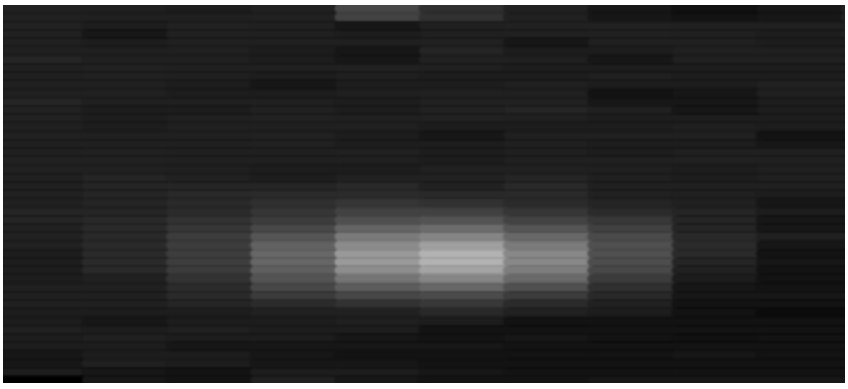

Figure 9: Image of the needle tip using the Hall-Effect sensor, with filtering.

Depth Readings

The depth readings from the Hall-Effect sensor can be displayed, using serial communication, as shown in Figure 10. The current measured depth, D of the needle tip is outputted, along with the current angle of the servo motor (in degrees) and the longitudinal location of the sensor in steps. The location of the needle tip is also printed, which is the location with the smallest depth, or also equivalently, the location of the strongest magnetic field out of the readings so far. To find the tip of the needle, the software locates the brightest spot in the image, which corresponds to the area with the largest magnetic field strength.

```
D (cm) = 2.63   angle = 61      position = 3    needle_depth = 2.14     needle_angle = 70       needle_position = 1
D (cm) = 2.14   angle = 62      position = 3    needle_depth = 2.14     needle_angle = 70       needle_position = 1
D (cm) = 2.14   angle = 63      position = 3    needle_depth = 2.14     needle_angle = 70       needle_position = 1
D (cm) = 2.08   angle = 64      position = 3    needle_depth = 2.08     needle_angle = 64       needle_position = 3
D (cm) = 1.91   angle = 65      position = 3    needle_depth = 1.91     needle_angle = 65       needle_position = 3
D (cm) = 1.86   angle = 66      position = 3    needle_depth = 1.86     needle_angle = 66       needle_position = 3
D (cm) = 1.72   angle = 67      position = 3    needle_depth = 1.72     needle_angle = 67       needle_position = 3
D (cm) = 1.77   angle = 68      position = 3    needle_depth = 1.72     needle_angle = 67       needle_position = 3
D (cm) = 1.81   angle = 69      position = 3    needle_depth = 1.72     needle_angle = 67       needle_position = 3
D (cm) = 1.91   angle = 70      position = 3    needle_depth = 1.72     needle_angle = 67       needle_position = 3
D (cm) = 2.02   angle = 71      position = 3    needle_depth = 1.72     needle_angle = 67       needle_position = 3
D (cm) = 2.21   angle = 72      position = 3    needle_depth = 1.72     needle_angle = 67       needle_position = 3
D (cm) = 2.63   angle = 73      position = 3    needle_depth = 1.72     needle_angle = 67       needle_position = 3
```

Figure 10: Serial printout of the depth of the needle as a function of position.

Final Image

From the numerical depth readings, the exact location of the needle tip can be passed to the Processing software to highlight that band in the image. Figures 11 and 12 below are examples of the final result. A red band is drawn at the location of the needle tip as determined by the Hall-Effect sensor. The two images also show the effect of the polarity of the magnetic field. If the magnet is rotated 180°, the magnetic field strength will be inverted, which will result in a dark spot in the image, which corresponds to a magnetic field in the opposite direction. The gray scale of each band can be adjusted to sense both polarities of the magnetic field. In this case, a gray band indicates no magnetic field, while a dark band indications the magnitude of the field in one direction, while a light band indicates the magnitude of the field in the opposite direction. A video showcasing the entire sweeping motion and image drawing is available on the web:

http://www.youtube.com/watch?v=CwmtKSEO_54

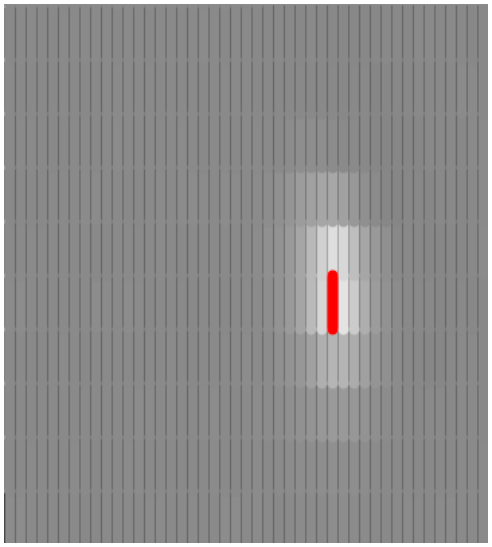

Figure 11: Image of the needle tip.

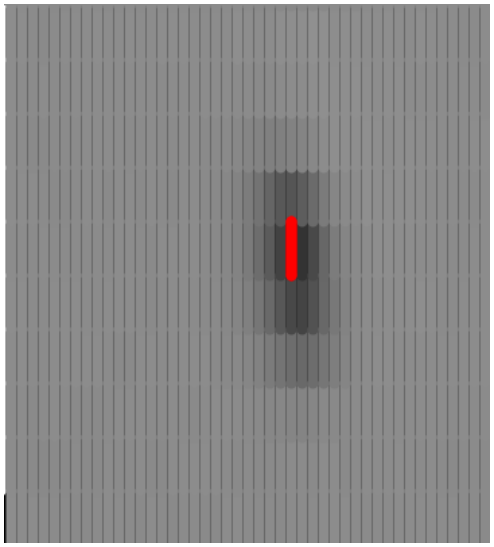

Figure 12: Image of the needle tip, with the magnet rotated 180°.

Image Comparison

An image created by the stud sensor is shown below in Figure 13 for comparison. The needle should be horizontal. Since the stud finder has a digital output, it will output a white band when the stud finder detects a change in the dielectric constant of the material. At a first glance, the image is very noisy, since the image is inconsistent and deviates from the actual shape of the horizontal needle. Since the stud finder is a digital sensor, it is unclear where in the in the series of white bands is the exact location of the needle.

The use of a Hall Effect sensor has much better performance than the original stud finder sensor as seen in Figures 11 and 12. In these images, the location of the tip of the needle is precisely pinpointed. Also the image is fairly noise-free.

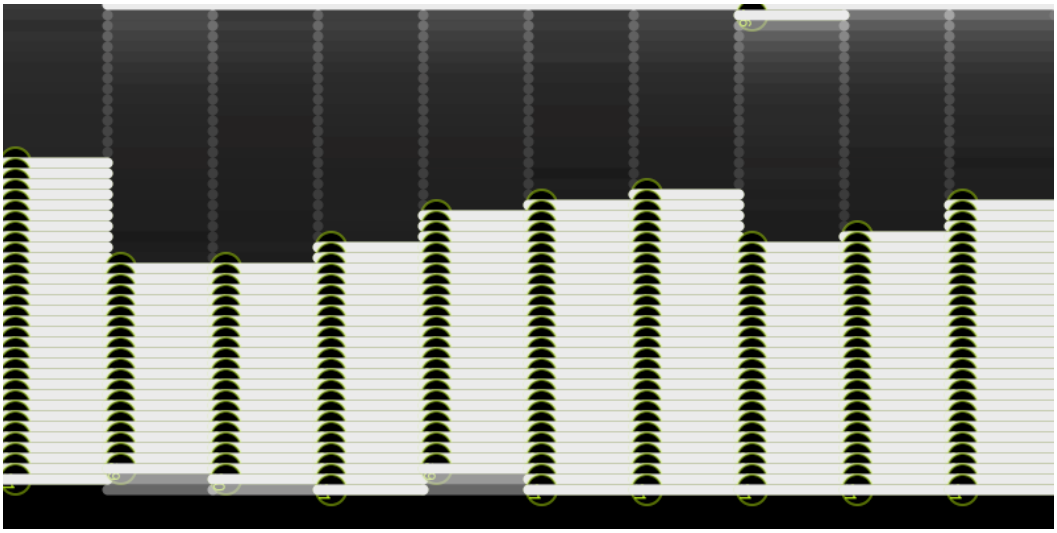

Figure 13: Plot of the sensing a horizontal needle using the stud finder.

Overall Improvements

The Hall-Effect sensor system that was implemented has many advantages over the existing stud sensor system. The major improvement is in reliability. The stud sensor must be calibrated to a surface every time it is turned on. The stud sensor must be exactly flush against the surface, or else it will read air pockets as changes in the dielectric constant, or calibrate to the wrong material.

During trials with the test bed, both the stud sensor and the phantom tissue must be flush against the plastic sheet, with no air pockets, in order to get reasonable results. Usually, many trials with the stud finder are required to produce reasonable images, due to the need to calibrate the stud finder, and the requirement that the stud finder be exactly flush against a flat surface. Separate images taken with the stud sensor for a given needle configuration can be very different, based on the calibration. Since calibration is a not a requirement for the Hall-Effect sensor, it can provide consistent results for every image.

Even with these limitations, the image from the stud sensor is noisy, and it is unclear where the precise location of the needle is. The Hall-Effect sensors have much better performance in noise reduction and pin pointing the location of the needle. The stud sensor can only detect the needle in two dimensions. The Hall-Effect sensor is able to also measure the extra dimension of depth. Table 1 highlights the advantages of the Hall-Effect Sensor over the stud sensor.

Stud Sensor	Magnet and Hall-Effect Sensor
Relatively expensive (~ $20/sensor)	Cheap (~ $4/sensor)
Needs to be calibrated to the flesh.	Magnetic fields pass through the flesh easily.
Can only work flush against a flat surface.	Does not need to be placed against a surface.
Noisy images.	Filtering methods efficient in noise reduction.
Digital sensor: binary data, exact position unclear.	Analog sensor: more resolution.
Detection on a plane at best.	Can detect in three dimensions.

Table 1: Comparison between the current setup and the proposed setup.

Discussion

The calibration methods may have precision error. The use of a ruler to gather data points limits precision to a millimeter. Also, there is uncertainty in the measured data points, due to errors at the small scales of measurement. The fitted curve is fairly accurate, but does not fit the data points exactly. Perhaps the calibration should be done again for more accurate coefficients. This calibration curve is different for stronger and weaker magnets. There is also a slight manufacturing difference between each sensor. Thus, for optimum precision, each Hall Effect sensor should be individually calibrated to a certain magnet.

However, the major issue is that the depth readings are not very accurate, due to the difficulty in modeling a non-uniform magnetic field. The actual distance may be different due to the orientation of the magnet. However, there is a considerable improvement in sensing the needle in two dimensions.

The combination of analog and digital filtering methods were able to improve the performance of the Hall-Effect sensor by removing almost all of the white noise produced by the sensor. This contrasts with the data from the stud sensor, which were noisy.

Conclusion:

Limitations of magnetic field sensing are the size and field strength of the magnet and the short detection range of the Hall-Effect sensors. Also, the needle must be within 2 centimeters in order for the Hall-Effect sensor to detect it. However, there are huge gains in the quality of the image.

If this project was allocated a larger budget, there can be much better results. Access to high-end ultrasound imaging may improve sensing considerably. The scope of this project is also limited by time. Since this project was completed by an undergraduate working

independently over the summer the results were limited. However, if more time and resources were allocated, there can be more room for many improvements to magnetic field sensing.

Hall Effect sensors with higher sensitivity can be purchased, which can have a longer detection range. Also, a stronger magnet can be acquired, which can also extend the detection range. Also, if there was some way to magnetize the entire needle, the Hall Effect sensor can detect the entire length of the needle, not just the tip. Also, with a linear magnetic source, the tip can be approximated as a magnetic monopole (assuming the needle is long enough), meaning there will be a fairly radial and uniform magnetic field, which will improve accuracy.

Since measuring the distance to the needle is inconsistent, a lot more improvements can be made on improving the distance reading. Implementing a Kalman filter may improve the sensor readings.

Also, the dipole nature of the magnet can be used to measure the orientation of the magnet, if an array of sensors is used. In the current setup, the needle remains stationary, while the sensor is actuated across the workspace of the needle. An array of sensor with sufficient range will allow the needle to move, while stationary sensors track the trajectory of the needle in real-time, instead of the current setup where the needle is stationary and moving sensors track the position of the needle.

Acknowledgements:

- Professor Ken Goldberg and Dr. Jur van der Berg for supporting and overseeing my work.
- Siamak Faridani and Melissa Goldstein for their advice.
- The Berkeley Center for New Media and the Automations Sciences Laboratory for providing resources.

References:

[1] R.J. WebsterIII, J.S. Kim, N.J. Cowan, G.S. Chirikjian, and A.M. Okamura, "Nonholonomic modeling of needle steering," *The International Journal of Robotics Research*, vol.25, no.5-6, pp. 509–525, 2006.

[2] K.B. Reed, V. Kallem, R. Alterovitz, K. Goldberg, A.M. Okamura, and N.J. Cowan, "Integrated planning and image-guided control for planar needle-steering," in *Proc. IEEE Conf. Biomedical Robotics*, October 2008, pp. 819–824.